helix B.) The first residue in each helix is numbered 1; thus, A1 refers to the first residue in helix A. Amino acids are represented by their single-letter, uppercase abbreviations, and McLachlan (*12*) positions are in lowercase bold. When the crystalline dimer is referred to, the helices from one monomer are labeled with plain letters and those from the other are labeled with a prime.
9. D. M. Shotton, B. Burke, D. Branton, *J. Mol. Biol.* **131**, 303 (1979); D. W. Speicher, J. S. Morrow, W. J. Knowles, V. T. Marchesi, *Proc. Natl. Acad. Sci. U.S.A.* **77**, 5673 (1980).
10. Unlike a number of the other spectrin repetitive motifs, segment 14 of the *Drosophila* α chain contains no Pro in the region between helix B and C, so that a continuous BC helix is possible. Furthermore, we note that the BC loop is variable in length from segment to segment; in α-spectrin segment 9, it contains an entire Src homology 3 domain.
11. T. Blundell, D. Barlow, N. S. Borkalsoti, J. Thornton, *Nature* **306**, 281 (1983).
12. A. D. McLachlan and M. Stewart, *J. Mol. Biol.* **98**, 293 (1975).
13. D. W. Banner, M. Kokkinidis, D. Tsernoglou, *ibid.* **196**, 657 (1987); E. K. O'Shea, J. D. Klemm, P. S. Kim, T. Alber, *Science* **254**, 539 (1991); B. Lovejoy *et al.*, *ibid.* **259**, 1288 (1993).
14. C. Chothia, M. Levitt, D. Richardson, *Proc. Natl. Acad. Sci. U.S.A.* **74**, 4130 (1977).
15. F. H. C. Crick, *Acta Crystallogr.* **6**, 89 (1953).
16. W. T. Tse *et al.*, *J. Clin. Invest.* **86**, 909 (1990).
17. D. W. Speicher *et al.*, *J. Biol. Chem.* **268**, 4227 (1993); L. Kotula, T. M. DeSilva, D. W. Speicher, P. J. Curtis, *ibid.*, p. 14788.
18. J. Palek, in *Hematology*, W. Williams, E. Beutler, A. Erslev, M. Lichtman, Eds. (McGraw-Hill, New York, ed. 4, 1990), pp. 569–581.
19. Corresponding to Asp B10 in *Drosophila* α14.
20. T. L. Coetzer *et al.*, *J. Clin. Invest.* **88**, 743 (1991).
21. Corresponding to Arg C8 in *Drosophila* α14.
22. R. R. Dubreuil *et al.*, *J. Cell Biol.* **109**, 2197 (1989).
23. Single-letter abbreviations for the amino acid residues are as follows: A, Ala; C, Cys; D, Asp; E, Glu; F, Phe; G, Gly; H, His; I, Ile; K, Lys; L, Leu; M, Met; N, Asn; P, Pro; Q, Gln; R, Arg; S, Ser; T, Thr; V, Val; W, Trp; and Y, Tyr.
24. T. J. Byers, E. Brandin, R. A. Lue, E. Winograd, D. Branton, *Proc. Natl. Acad. Sci. U.S.A.* **89**, 6187 (1992).
25. Crystals (in space group $P2_12_12$) were grown at room temperature with vapor diffusion against a well solution containing 10% polyethylene glycol (PEG) 400, 1 M ammonium acetate, 50 mM MES (4-morpholineethane sulfonic acid), pH 6.0. The starting mixture contained a 1:1 mixture of protein (20 mg/ml) and well solution. The polypeptide used for crystallization (originally called B14) was cleaved from a fusion protein generated in *Escherichia coli* as described (*6*). The mercury derivative was obtained by soaking crystals for 2 days in stabilization buffer (14% PEG 400, 1.2 M ammonium acetate, pH 6.0) saturated in CH_3HgCl, followed by a 1-hour backsoak. To prepare the K_3OsCl_6 derivative, the ammonium acetate in the stabilization buffer was exchanged for 1.2 M sodium acetate, and the crystals were soaked for 1 day in stabilization buffer containing 1 mM K_3OsCl_6. Data were collected with a Siemens area detector on an Elliot GX-13 rotating anode generator (Avionics, Borehamwood, United Kingdom). CuKα radiation was provided by a Frank's double-focusing mirror assembly [S. C. Harrison, *J. Appl. Crystallogr.* **1**, 84 (1968)]. Data collection was controlled as described by M. Blum, P. Metcalf, S. C. Harrison, and D. C. Wiley [*J. Appl. Crystallogr.* **20**, 235 (1987)], and the data were processed by the XDS package of W. Kabsch [*ibid.* **21**, 916 (1988)]. Anomalous dispersion measurements were included in calculations of the phasing for the CH_3HgCl derivative. The Hg atom positions for the CH_3HgCl derivative were determined from a difference Patterson function. There were two sites in the asymmetric unit, and each site splits into two subsites, 3 Å apart. The K_3OsCl_6 derivative was solved from a difference Fourier synthesis phased on the CH_3HgCl derivative. There is one site per asymmetric unit. Heavy-atom parameters were refined, and initial phases were calculated with the program HEAVY [T. C. Terwilliger and D. Eisenberg, *Acta Crystallogr. Sect. A* **39**, 813 (1983)].
26. Low-resolution data (3 Å) were collected at room temperature with unit cell a = 47.91 Å, b = 48.70 Å, c = 105.29 Å for native I and two derivatives. High-resolution data (2 and 1.8 Å) were collected at cryogenic temperature (−160°C) (native II and III; before data collection crystals were soaked in 25% PEG 400 and 1.2 M ammonium acetate, pH 6.0, for one day) with unit cell a = 46.80 Å, b = 47.22 Å, and c = 104.43 Å. The model built into the map was partially refined, with XPLOR [A. T. Brunger, *XPLOR Manual, Version 3.1* (Yale University, New Haven, CT, 1992); *Acta Crystallogr. Sect. A* **46**, 585 (1990)] against the native I (room temperature) data set. We then used the model to determine phases in the native II data set by refining six rigid segments in the resolution range of 12 to 3 Å ($R = \Sigma|F_{obs} - F_{calc}|/\Sigma F_{obs} = 0.36$, where F_{obs} and F_{calc} are the observed and calculated structure-factor amplitudes, respectively). A randomly selected 10% subset of the data was set aside for use in "free R factor" calculations. [A. T. Brunger, *Nature* **355**, 472 (1992)]. The results of the rigid-body search were manually adjusted in $2F_o - F_c$ and $F_o - F_c$ maps, and the resolution was extended to 2 Å in several stages. Cycles of simulated annealing refinement against 6 to 2 Å resolution data, alternated with manual adjustment and the addition of ordered water molecules, gave an R factor of 0.21 (R_{free} = 0.34). A still better low-temperature data set (Native III), extending to 1.8 Å resolution, then became available. Simulated annealing was used to refine against these data, first at 2 Å and then at 1.8 Å resolution (R = 0.23, R_{free} = 0.32); further refinement with TNT [D. E. Tronrud, L. F. TenEyck, B. W. Matthews, *Acta Crystallogr. Sect. A* **43**, 489 (1987)] yielded an R factor of 0.203 (R_{free} = 0.304, 6 to 1.8 Å, $F > 2\sigma$, 91% complete), with excellent geometry (σ_{bond} = 0.017 Å; σ_{angle} = 2.2°). The final model had 107 ordered residues in each monomer (including one from the NH_2-terminal cloning artifact) and a total of 156 ordered water molecules in the asymmetric unit. The coordinates of the refined model have been deposited in Brookhaven Protein Data Bank.
27. We thank W. Stafford for equilibrium sedimentation analyses. Supported by National Institutes of Health grants CA 13202 (S.C.H.) and HL 17411 (D.B.).

30 July 1993; accepted 19 October 1993

A Covalent Enzyme-Substrate Intermediate with Saccharide Distortion in a Mutant T4 Lysozyme

Ryota Kuroki,* Larry H. Weaver, Brian W. Matthews†

The glycosyl-enzyme intermediate in lysozyme action has long been considered to be an oxocarbonium ion, although precedent from other glycosidases and theoretical considerations suggest it should be a covalent enzyme-substrate adduct. The mutation of threonine 26 to glutamic acid in the active site cleft of phage T4 lysozyme (T4L) produced an enzyme that cleaved the cell wall of *Escherichia coli* but left the product covalently bound to the enzyme. The crystalline complex was nonisomorphous with wild-type T4L, and analysis of its structure showed a covalent linkage between the product and the newly introduced glutamic acid 26. The covalently linked sugar ring was substantially distorted, suggesting that distortion of the substrate toward the transition state is important for catalysis, as originally proposed by Phillips. It is also postulated that the adduct formed by the mutant is an intermediate, consistent with a double displacement mechanism of action in which the glycosidic linkage is cleaved with retention of configuration as originally proposed by Koshland. The peptide part of the cell wall fragment displays extensive hydrogen-bonding interactions with the carboxyl-terminal domain of the enzyme, consistent with previous studies of mutations in T4L.

Among the glycosidases much detailed structural information is available for the lysozymes (*1–3*), but their mechanism (or mechanisms) of action has remained contentious (*4–8*). In an attempt to create metal binding sites, as was done successfully for human lysozyme (*9*), a number of acidic groups were introduced. One such substitution, $Thr^{26} \rightarrow Glu$ (T26E), produced an enzyme that was inactive at neutral pH. This result was unexpected because Thr^{26} is located within the active site cleft of T4L but was thought not to be critical for catalysis because some other amino acids are tolerated at this position (*10*).

Mutant T26E was constructed and purified (*11*). More than 30 cycles of Edman degradation showed the NH_2-terminal sequence of the major component (*11*) to be that predicted for the T26E mutant. A mass of 19,548 daltons (T26E + 918) was determined with electron ion spray mass spectrometry. The major component of *E. coli* cell wall, (NAM-NAG)-LAla-DGlu-DAP-DAla, has a molecular weight of 940 (NAM, *N*-acetyl/muramic acid; NAG, *N*-acetyl/glucosamine; and DAP, diamino-

Institute of Molecular Biology, Howard Hughes Medical Institute, and Department of Physics, University of Oregon, Eugene, OR 97403.

*Present address: Kirin Brewery Company, Ltd., Central Laboratories for Key Technology, 1-13-5, Fukuura, Kanazawa-ku, Yokohama 236, Japan.
†To whom correspondence should be addressed.

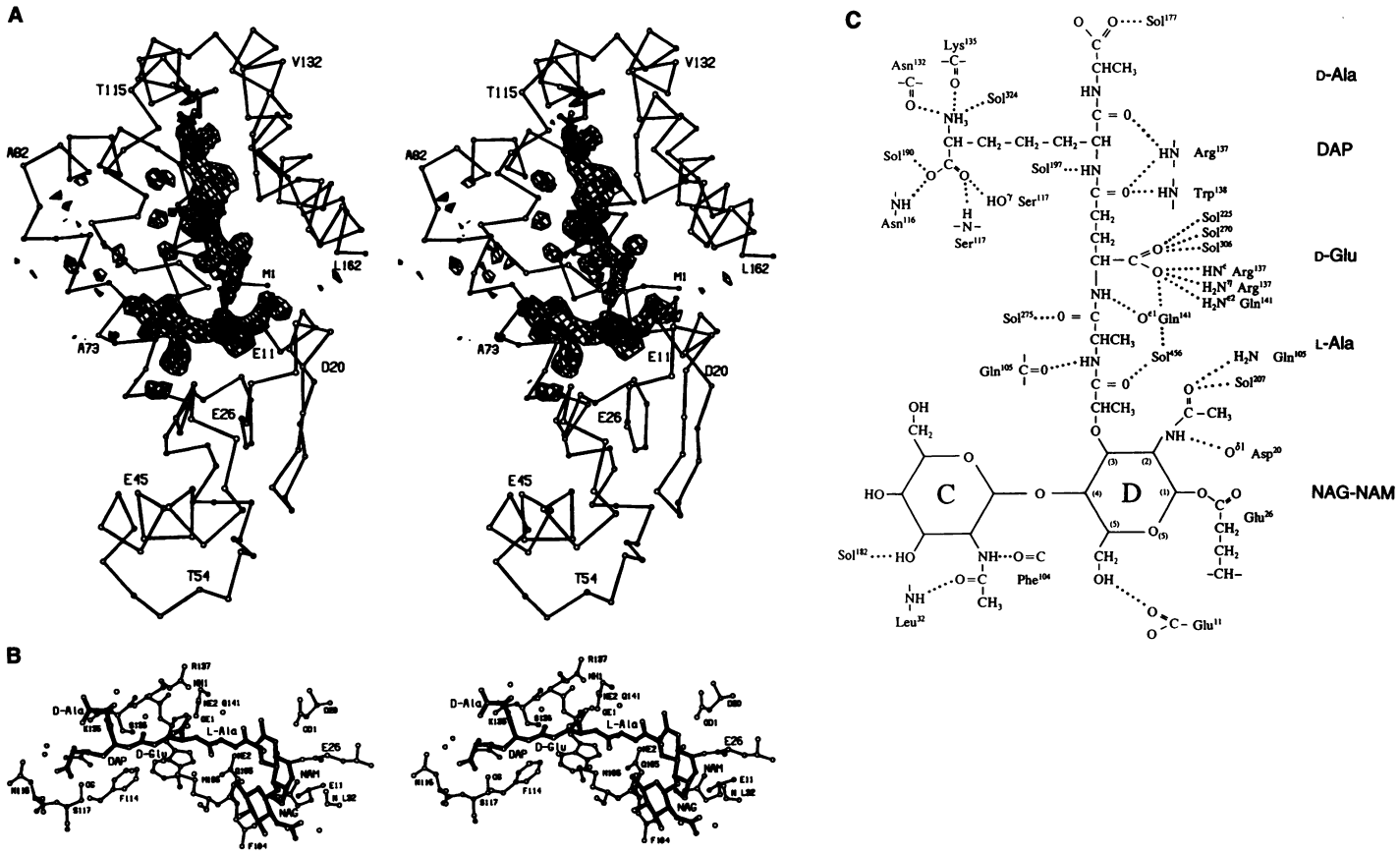

Fig. 1. (**A**) Map showing difference in electron density between the adduct and wild-type T4L. Amplitudes are ($F_{adduct} - F_c$) where F_{adduct} is the amplitude observed for the adduct and F_c is the amplitude calculated for the protein model alone. After a screen of a variety of conditions (*24*), a single crystal was obtained from 0.1 M tris-HCl, 0.2 M sodium acetate, and 30% PEG 3000 (pH 7.5). The space group is $P2_12_12$ with cell dimensions a = 50.9 Å, b = 67.3 Å, and c = 49.6 Å. We measured 11,889 reflections (*25*) to 1.9 Å resolution (85% complete) with an average disagreement of 5.5% on intensities. With the wild-type structure (*13*) as a model, the structure was solved by molecular replacement. Refinement (*15*) of the protein part alone (that is, without solvent and without saccharide) reduced the R value to 22.1% at 2.0 Å resolution. Phases from this model were then used to calculate the electron density map shown in Fig. 1A. The map (resolution 2.0 Å) contoured at 3.0 σ is shown with the adduct and the α carbon backbone of the protein superimposed. Density corresponding to the disaccharide extends horizontally within the active site cleft. The peptide part extends vertically in a shallow groove between two α helices of the COOH-terminal domain (*26*). After inclusion of the adduct and 164 solvent molecules, further refinement reduced the R value to 16.3% at 1.9 Å resolution (*14*). (**B**) Stereo view of the peptidoglycan (thicker bonds) bound to T4L (thinner bonds), rotated about 90° from the view in (A). (**C**) Schematic view indicating probable hydrogen-bonding interactions (dotted) between T4L and the peptidoglycan.

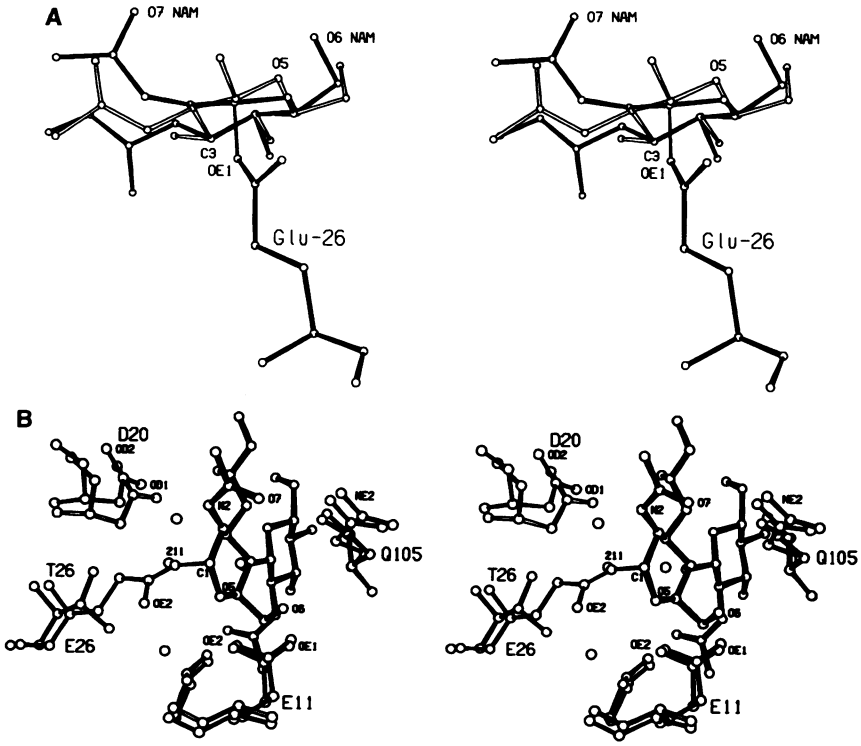

Fig. 2. (**A**) Superposition of NAM from the D subsite (solid bonds) on NAG from the C subsite (open bonds). The NAM moiety is covalently linked to Glu^{26} (solid bonds). (**B**) Stereo view showing the superposition of wild-type lysozyme (open bonds) on the complex of T26E (thin solid bonds) with the covalent adduct (thick solid bonds). Water molecule 211 (SOL^{211}) in the wild-type structure essentially superimposes on $O^{\epsilon 1}$ of Glu^{26} in the adduct. Three solvent molecules that are within 5 Å of carbon C-1 in the structure of the adduct are also shown.

pimelic acid) (*12*). Allowing 18 daltons for the loss of a water of condensation and 4 daltons for the difference between the formula molecular weight of the protein and its actual state of ionization, the purified material appeared to correspond to a covalent adduct between the mutant T26E and the saccharide.

The adduct was crystallized from 0.2 M sodium acetate, 30% polyethylene glycol (PEG) 3000, and 0.1 M tris-HCl (pH 7.5) in a form nonisomorphous with wild type (Fig. 1) (*13*). The structure of the protein part was determined by molecular replacement with the wild-type enzyme as a search model. A difference electron density map (Fig. 1A) had clear density in the region expected for a bound peptidoglycan. Refinement (*14, 15*) showed that the additional density was consistent with a disaccharide of NAG-NAM bound in subsites C and D (*1–3*). It also showed that a peptide of LAla-DGlu-DAP-DAla extended across an open groove on the surface of the molecule between α helices 108 to 113 and 126 to 134 (Fig. 1, B and C) as expected on the basis of earlier studies of low-activity mutants of T4L (*16*). Interactions between the peptide moiety and the enzyme are critical for catalysis because T4L, unlike hen egg white lysozyme (HEWL), will not hydrolyze oligosaccharides such as chitin that lack a peptide substituent (*17*). These interactions also explain why residues in or close to the peptide binding site, such as Gln^{105}, Met^{106}, Phe^{114}, Ser^{117}, Ser^{136}, and Trp^{138}, are relatively intolerant to substitution (*10*).

Previously, no saccharide had been observed in the D subsite of T4L. Consistent with model-building experiments (*18*), we find the NAM moiety in this subsite to be distorted (Fig. 2A). The NAM ring is in the α-conformation and adopts a sofa form with atoms C-1, C-2, C-4, C-5, and O-5 nearly coplanar [0.07 Å root-mean-square (rms) discrepancy from coplanar]. In the full chair configuration, as in subsite C, the rms discrepancy from coplanar of the same five atoms is 0.25 Å. The *N*-acetyl group is shifted so as to make hydrogen bonds with Asp^{20} and Gln^{105}, and, as a result, the nitrogen is in the plane of the sofa atoms. Also, the normally equatorial hydroxymethyl group at C-5 is shifted toward the axial position where it makes a favorable hydrogen bond to Glu^{11}. Thus, these multiple interactions with the enzyme seem to favor the distorted form that is observed when the saccharide is bound in subsite D. A similar distortion and interactions favorable to that distortion were seen in the complex of HEWL and NAM-NAG-NAM (*5, 8*).

On the basis of the structure of the covalent adduct, it is presumed that Glu^{11} donates a proton to the O-5 of NAM in subsite D and Glu^{26} is optimally located for nucleophilic attack on the C-1 carbon, leading to the observed covalent linkage (Fig. 3A). At pH 3.0 and 37°C the resultant adduct is cleaved within 1 hour. This is illustrated in Fig. 3A, although the role of Glu^{11} in promoting the attack of the water molecule is hypothetical. Nucleophilic attack by a carboxylate in glycosyl bond cleavage (Fig. 3A) is well established for β-glucosidase (*19*) and β-galactosidase (*20*). Because the observed adduct is distorted toward an oxocarbonium ion–like conformation, it suggests that the same enzyme-substrate interactions stabilize the transition state and prevent relaxation of the covalent glycosyl-enzyme intermediate to a stable ground-state conformation. Therefore, the deglycosylation step should be rapid, assuming free access by an acceptor group to the strained ring. In the case of the present adduct there is a well-ordered water molecule hydrogen bonded to the *N*-acetyl group and to Glu^{11} (Fig. 2B). These hydrogen-bonding interactions, plus $O^{\epsilon 2}$ of Glu^{26}, apparently restrict access of the solvent to C-1. The overall mechanism shown in Fig. 3A is consistent with the double displacement reaction envisaged for "configuration retaining" glycosidases in which a glycosyl-enzyme is formed and subsequently hydrolyzed (*21, 22*). The mechanism of action of T4L itself is unclear (Fig. 3B).

If the enzyme-adduct complex is superimposed on wild-type T4L (Fig. 2B), $O^{\epsilon 1}$ of Glu^{26} in the adduct superimposes almost exactly on a solvent molecule (SOL^{211}) that is bound between Thr^{26} and Asp^{20} in the native structure. Consideration of hydrogen bonding (Fig. 3B) suggests that the lone pair of the bound solvent is directed toward the site occupied by the C-1 carbon. This suggests that in the wild-type enzyme this solvent molecule might attack in what would be a single displacement reaction (Fig. 3B), inverting the anomeric configuration from equatorial in the substrate to axial in the product of hydrolysis. The hypothesis that solvent attack occurs from

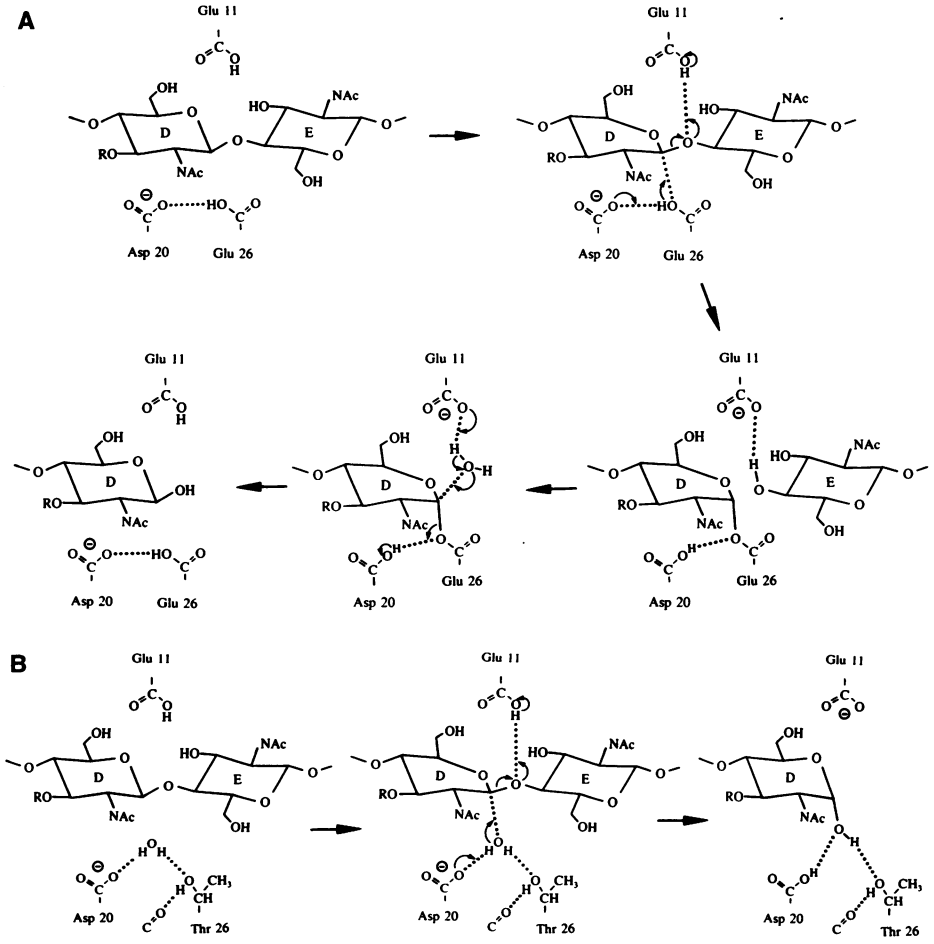

Fig. 3. (**A**) Proposed steps leading to the adduct formed by T26E lysozyme and its subsequent breakdown. If the active site of phage T4L is superimposed on that of HEWL (*27, 28*), Glu^{11} of T4L superimposes on Glu^{35} of HEWL. In this superposition Asp^{20} of T4L is in the same vicinity as Asp^{52} of HEWL, but the position of Asp^{52} in HEWL corresponds more closely to Thr^{26} of T4L than to Asp^{20} [see figure 2 of (*27*) and table 3 of (*28*)]. (**B**) One possible mechanism of action of wild-type T4L, based on analogy with the covalent adduct. Other mechanisms are also consistent with the available data (see text).

the α side of the saccharide in native T4L predicts that the anomeric configuration of the substrate be inverted in the product. This is difficult to prove because the appropriate substrate for T4L is complex and difficult to synthesize. In contrast, HEWL is known to retain anomeric configuration (*23*). Therefore, the mechanism for T4L shown in Fig. 3B is necessarily different from that commonly accepted for HEWL (*1*, *4*, *5*).

Thus, the mutant lysozyme T26E could be an example of glycosidases that cleave with overall retention of configuration by a double displacement mechanism (*21*, *22*). At the same time, the presence of protein-substrate interactions that stabilize a sugar ring conformation similar to an oxocarbonium ion–like transition state can be taken as evidence that the mechanism of action of the mutant and of the wild-type T4L itself include elements similar to those originally postulated by Phillips for HEWL (*1*, *4*, *5*).

REFERENCES AND NOTES

1. C. C. F. Blake *et al.*, *Nature* **206**, 757 (1965).
2. B. W. Matthews and S. J. Remington, *Proc. Natl. Acad. Sci. U.S.A.* **71**, 4178 (1974).
3. M. G. Grütter, L. H. Weaver, B. W. Matthews, *Nature* **303**, 828 (1983).
4. D. C. Phillips, *Proc. Natl. Acad. Sci. U.S.A.* **57**, 484 (1967).
5. N. C. J. Strynadka and M. N. G. James, *J. Mol. Biol.* **220**, 401 (1991).
6. M. L. Sinnott, *Chem. Rev.* **90**, 1171 (1990); C. B. Post and M. Karplus, *J. Am. Chem. Soc.* **108**, 1317 (1986); B. A. Malcolm *et al.*, *Proc. Natl. Acad. Sci. U.S.A.* **86**, 133 (1989); L. W. Hardy and A. R. Poteete, *Biochemistry* **30**, 9457 (1991).
7. B. Svensson and M. Søgaard, *J. Biotechnol.* **29**, 1 (1993).
8. K. J. Lumb *et al.* [*FEBS Lett.* **296**, 153 (1992)] have suggested that a small fraction of complexes between $GLcNAc_4$ and $GlcNAc_6$ and the chicken lysozyme with the mutation $Asp^{52} \rightarrow Ser$ may exist as a covalent adduct.
9. R. Kuroki *et al.*, *Proc. Natl. Acad. Sci. U.S.A.* **86**, 6903 (1989); R. Kuroki, H. Kawakita, H. Nakamura, K. Yutani, *ibid.* **89**, 6803 (1992).
10. D. Rennell, S. E. Bouvier, L. W. Hardy, A. R. Poteete, *J. Mol. Biol.* **222**, 67 (1991).
11. D. C. Muchmore, L. P. McIntosh, C. B. Russell, D. E. Anderson, F. W. Dahlquist, *Methods Enzymol.* **177**, 44 (1989); A. R. Poteete, S. Dao-pin, H. Nicholson, B. W. Matthews, *Biochemistry* **30**, 1425 (1991). Standard purification was followed by cation exchange and reversed-phase chromatography. This showed three components, the largest of which (~75%) was the enzyme-substrate adduct (see text). The other two components were the free mutant enzyme (~15%) and an enzyme-saccharide-enzyme dimer (~10%).
12. J.-M. Ghuysen, *Bacteriol. Rev.* **32**, 425 (1968); K. H. Schleifer and O. Kandler, *ibid.* **36**, 407 (1972).
13. L. H. Weaver and B. W. Matthews, *J. Mol. Biol.* **193**, 189 (1987); J. A. Bell *et al.*, *Proteins* **10**, 10 (1991).
14. During refinement the bond lengths but not the bond angles within the saccharide rings were restrained. Within the *N*-acetyl group both bond lengths and angles were restrained. For the complete structure the rms deviations of bond lengths and bond angles from ideal were 0.016 Å and 2.8°, respectively. The rms discrepancy between the backbone atoms in wild-type lysozyme and the complex was 0.59 Å.
15. D. E. Tronrud, L. F. Ten Eyck, B. W. Matthews, *Acta Crystallogr. Sect. A* **43**, 489 (1987); D. E. Tronrud, *ibid.* **48**, 912 (1992).
16. M. G. Grütter and B. W. Matthews, *J. Mol. Biol.* **154**, 525 (1982).
17. H. B. Jensen, G. Kleppe, M. Schindler, D. Mirelman, *Eur. J. Biochem.* **66**, 319 (1976).
18. W. F. Anderson, M. G. Grütter, S. J. Remington, B. W. Matthews, *J. Mol. Biol.* **147**, 523 (1981).
19. I. P. Street, J. B. Kempton, S. G. Withers, *Biochemistry* **31**, 9970 (1992).
20. J. C. Gebler, R. Aebersold, S. G. Withers, *J. Biol. Chem.* **267**, 11126 (1992).
21. D. E. Koshland, *Biol. Rev.* **28**, 416 (1953).
22. J. B. Kempton and S. G. Withers, *Biochemistry* **31**, 9961 (1992).
24. J. Jancarik and S.-H. Kim, *J. Appl. Crystallogr.* **24**, 409 (1991).
23. F. W. Dahlquist, C. L. Borders, G. Jacobson, M. A. Raftery, *Biochemistry* **8**, 694 (1969).
25. R. Hamlin, *Methods Enzymol.* **114**, 416 (1985); X.-J. Zhang and B. W. Matthews, *J. Appl. Crystallogr.* **26**, 457 (1993).
26. Abbreviations for the amino acid residues are the following: A, Ala; C, Cys; D, Asp; E, Glu; F, Phe; G, Gly; H, His; I, Ile; K, Lys; L, Leu; M, Met; N, Asn; P, Pro; Q, Gln; R, Arg; S, Ser; T, Thr; V, Val; W, Trp; and Y, Tyr.
27. B. W. Matthews, M. G. Grütter, W. F. Anderson, S. J. Remington, *Nature* **290**, 334 (1981).
28. L. H. Weaver *et al.*, *J. Mol. Evol.* **21**, 97 (1985).

29. Coordinates have been deposited in the Brookhaven Protein Data Bank. We are grateful to W. A. Baase for help with preliminary thermodynamic and mass spectroscopic analyses; F. W. Dahlquist and E. Anderson for nuclear magnetic resonance analyses; S. Pepiot and J. A. Wozniak for technical help; and H. Yamada, S. J. Remington, and F. W. Dahlquist for helpful discussions. R.K. acknowledges the support of Kirin Brewery Company. Supported in part by grants from NIH (GM21967) and the Lucille P. Markey Charitable Trust.

20 August 1993; accepted 1 November 1993

Chromosome Condensation in *Xenopus* Mitotic Extracts Without Histone H1

Keita Ohsumi,* Chiaki Katagiri, Takeo Kishimoto

The contribution of histone H1 to mitotic chromosome condensation was examined with the use of a cell-free extract from *Xenopus* eggs, which transforms condensed sperm nuclei into metaphase chromosomes. When H1 was removed from the extract, the resultant metaphase chromosomes were indistinguishable from those formed in complete extract. Nucleosomal spacing was the same for both. Thus, H1 is not required for the structural reorganization that leads to condensed metaphase chromosomes in this egg extract.

During mitosis, genomic DNA is packaged into condensed chromosomes to facilitate its accurate segregation to daughter cells. Concomitant with mitotic chromosome condensation, histone H1 is highly phosphorylated (*1*), presumably by cdc2 kinase that triggers the transition from interphase to mitosis (*2*) and is partially localized on condensed chromosomes (*3*). Histone H1 helps to compact the 10-nm-diameter chromatin filament into a 30-nm fiber (*4*). Thus, H1 and its phosphorylation are thought to cause mitotic chromosome condensation (*5*). To examine the contribution of H1 to mitotic chromosome condensation, we used a cell-free system with amphibian (*Xenopus laevis*) egg extracts, in which sperm chromatin lacking H1 is remodeled to somatic chromatin and then transformed into condensed metaphase chromosomes (*6*).

Unfertilized eggs of *Xenopus* are arrested at the second meiotic metaphase. Cytoplasmic extracts prepared from these eggs can induce nuclear membrane breakdown, chromosome condensation, and spindle formation (*6–9*). When sperm nuclei deprived of the plasma and nuclear membranes are incubated in the mitotic extract, they decondense in a few minutes (*9*, *10*). During this time, sperm-specific basic proteins are selectively removed from sperm DNA and replaced by somatic-type core histones and H1, which are absent from sperm nuclei but stored in the extract (*10–12*). Both of these processes are mediated by nucleoplasmin (*11–13*). The decondensed chromatin is then transformed into condensed metaphase chromosomes after incubation for a further 90 min (*8*, *9*). This condensation is thought to be similar to that imposed on somatic interphase nuclei when incubated in the egg extract (*6*).

Although the type of H1 commonly found in somatic cells is not found in amphibian eggs (*14*, *15*), a subtype termed H1X is found in the nuclei of eggs and early embryos up to the late blastula stage of anuran amphibians (*10*). This subtype is encoded by the B4 mRNA, whose sequence is similar to those of other subtypes of H1 (*16*).

We used antibodies to H1X to immunodeplete the egg extracts (*17*) (Fig. 1A). In both H1X-depleted and normal extracts, sperm nuclei were similarly transformed

K. Ohsumi and T. Kishimoto, Laboratory of Cell and Developmental Biology, Faculty of Biosciences, Tokyo Institute of Technology, 4259 Nagatsuta, Midori-ku, Yokohama 227, Japan.
C. Katagiri, Division of Biological Sciences, Graduate School of Science, Hokkaido University, Sapporo 060, Japan.

*To whom correspondence should be addressed.

A covalent enzyme-substrate intermediate with saccharide distortion in a mutant T4 lysozyme

R Kuroki, LH Weaver and BW Matthews

Science **262** (5142), 2030-2033.
DOI: 10.1126/science.8266098